Phase diagrams of random-field Ising systems

1994 J. Phys. A: Math. Gen. 27 1525

(http://iopscience.iop.org/0305-4470/27/5/017)

J. Phys. A: Math. Gen. 27 (1994) 1525–1532. Printed in the UK

Phase diagrams of random-field Ising systems

Michael R Swift†, Amos Maritan‡, Marek Cieplak†§ and Jayanth R Banavar†

† Department of Physics and Materials Research Laboratory, The Pennsylvania State University, 104 Davey Laboratory, University Park, PA 16802, USA

‡ Dipartimento di Fisica, Universita di Padova, Padova, Italy

§ Institute of Physics, Polish Academy of Sciences, 02-668 Warsaw, Poland

Received 27 October 1993

Abstract. We show that the random-field Ising model may be tuned to obtain two distinct scenarios of phase diagram topology. Explicit evidence for this is presented in a numerically exact analysis in three dimensions and on a Bethe lattice, which allows us to investigate the effects of temperature, coordination number, and asymmetry in the field distribution.

1. Introduction

The Ising model in a random magnetic field provides a convenient theoretical framework for exploring the effects of randomness on phase transitions [1]. On the experimental front, certain classes of randomly dilute antiferromagnets [2], the phase separation of binary fluids in porous media [3] and the liquid–vapour critical point in porous media [4] are all believed to be realizations of the random-field Ising model (RFIM) [5]. The RFIM has a Hamiltonian

$$H = -J \sum_{\langle i,j \rangle} S_i S_j - \sum_i h_i S_i \tag{1}$$

where the fields are usually distributed symmetrically around zero either in a Gaussian or a bimodal fashion. In both cases, the strength of the random-field distribution is characterized by the root mean square fluctuations, $h_R = \langle h_i^2 \rangle^{1/2}$.

In this paper, we show that one may tune the RFIM to obtain either of two distinct scenarios of phase transitions. We find explicit evidence for this in the RFIM in three dimensions, for which we determine the ground states exactly for systems size up to 32^3 spins. Our results are supported by a numerically (and in one case analytic) *exact* analysis of the RFIM on a Bethe lattice which, surprisingly, yields a rich variety of phase diagram topologies.

In the literature, the phase diagram of the RFIM in the temperature T–h_R plane is of two types, as shown in figures 1(*a*) and (*b*). A mean-field analysis for a Gaussian distribution of fields [6], the bimodal model on a Bethe lattice with coordination number $z = 3$ [7], renormalization group analysis [8], some Monte Carlo simulations [9] and scaling theories of the RFIM [10] all find or postulate that the transition from a disordered to an ordered phase remains continuous down to $T = 0$ (figure 1(*a*)). On the other hand, high T series analysis [11], Monte Carlo simulations due to Young and Nauenberg [12] and mean-field analysis for a bimodal distribution of fields [13] are suggestive of a tricritical point in the

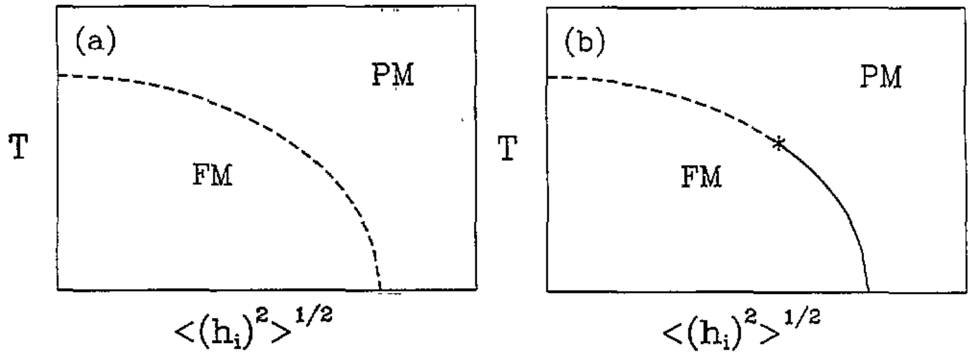

Figure 1. Phase diagrams in the T–h_R plane showing the boundary between the paramagnetic and ferromagnetic phases. In (*a*) the transition remains continous down to $T = 0$ while in (*b*) it becomes first order for sufficiently large h_R. The asterisk denotes a tricritical point.

T–h_R phase diagram (figure 1(*b*)) with the transition becoming first order for sufficiently strong fields [14].

The nature of criticality is expected to be different in these two scenarios. In the former case, figure 1(*a*), renormalization group ideas indicate that the transition is governed by a $T = 0$ fixed point: the basic competition at criticality is between the ordering tendency of the exchange interaction and the disordering effect of the field. Novel predictions of this scaling picture [10] include a divergence of relaxation times as the transition is approached and a violation of the standard hyperscaling relation. In the second scenario, however, there is no scope for a $T = 0$ fixed point as the transition becomes first order at low T. As a consequence, fluctuations due to both the random field and the temperature are expected to play a role at criticality.

On general thermodynamic grounds, tricritical points, such as the one in figure 1(*b*), arise out of the confluence of three critical lines—three distinct thermodynamic phases become critical simultaneously. It is thus natural to view the RFIM in an extended parameter space. For this reason, we consider the Ising model with a generalized bimodal field distribution

$$P(h_i) = p\delta(h_i - h_0) + (1-p)\delta(h_i + h_1) \tag{2}$$

where the symmetric case corresponds to $p = \frac{1}{2}$. The two parameters of the distribution, h_0 and h_1, are taken to be independent variables—when $h_0 \neq h_1$, odd moments are introduced into the field distribution.

Our results are best described, first, within the framework of Ising spins sitting on a Bethe lattice. The fluctuations in the random field can be treated exactly within this formalism. This system was first studied by Bruinsma [7] for a coordination number $z = 3$ and in the restricted space $p = \frac{1}{2}$ and $h_0 = h_1$. We have extended his work to investigate the effects of T, z and also asymmetry in the field distribution. Following [7], by introducing an effective field, x_n, which acts on the uppermost site of an nth generation branch, all thermodynamic properties can be calculated exactly once the fixed-point distribution of the x's, $W_\infty(x)$, has been determined. The hierarchical structure of the Bethe lattice gives rise to a functional recursion relation for $W_n(x)$,

$$W_{n+1}(x) = \int \mathrm{d}h\, P(h) \int \prod_{i=1}^{z-1} \mathrm{d}x_i\, W_n(x_i)\delta\Big(x - h - \sum_{i=1}^{z-1} g(x_i)\Big) \tag{3}$$

where

$$g(x) = \frac{1}{2\beta} \ln \left(\frac{\cosh \beta(x+1)}{\cosh \beta(x-1)} \right)$$

is a T-dependent function ($\beta = J/T$). Once the fixed point distribution has been determined, the interior spin magnetization follows from the integrals

$$m = \int \mathrm{d}x\, \mathrm{d}y\, W_\infty(x) W_\infty(y) \tanh \beta(x + g(y)) \tag{4}$$

over this distribution.

Bruinsma [7] showed that there was no tricritical point for $z = 3$ and $h_0 = h_1$. Our extension of the phase diagram in the parameter space T–h_0–h_1 is shown in figure 2(a). The $T = 0$ analysis of Bruinsma revealed Griffiths-type singularities [15] corresponding to the flipping of finite clusters of spins. These $T = 0$ singularities are not present at non-zero temperatures and have been omitted from the phase diagram. Figure 2(a) is an extension of figure 1(a) viewed in the enlarged parameter space of equation (2).

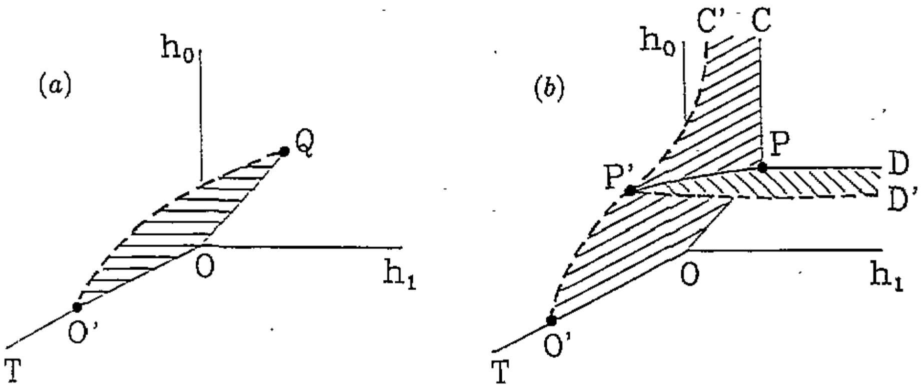

Figure 2. Phase diagrams, corresponding to figures 1(a) and 1(b), in the space T–h_0–h_1. The hatched surfaces denote first-order transitions where the magnetization varies discontinously while the broken curves are lines of critical points. In (a) there is a single critical line extending from the pure system critical point, O′, to the zero-temperature plane at Q. Figure 2(b) shows that the tricritical point, P′, present in figure 1(b), arises from the intersection of three critical lines O′P′, C′P′ and D′P′. At low T, there are three distinct phases separated by first-order transitions.

It is straightforward to show that for $z = \infty$, a different scenario corresponding to figure 1(b) is obtained. Inserting the fixed-point distribution $W_\infty(x)$ from equation (3) into equation (4) and integrating over x gives

$$m = \int \mathrm{d}h\, P(h) \int \prod_{i=1}^{z} \mathrm{d}x_i\, W_\infty(x_i) \tanh \beta \left(h + \sum_{i=1}^{z} g(x_i) \right). \tag{5}$$

In the limit $z \to \infty$, performing the integrals over the x_i's leads to the replacement of the sum in equation (5) by $zg(\bar{x})$, where $\bar{x}$ is the mean value of x_i. As $g(x_i)$ is the effective interaction between two neighbouring sites, $g(\bar{x}) = Jm$, where m is the magnetization. Thus, equation (5) takes the form

$$m = \int \mathrm{d}h\, P(h) \tanh \beta(m+h) \tag{6}$$

where we have put $J = 1/z$ to ensure a well defined thermodynamic limit. This equation for m is the same as that obtained for an infinite range RFIM—a model amenable to exact solution [6, 13]. The resulting phase diagram is shown in figure 2(*b*). A tricritical point is now present (the plane $h_0 = h_1$ corresponds to figure 1(*b*)) and two new sheets of first-order transitions ending in lines of critical points are obtained. Within this mean-field limit, the three phases giving rise to the tricritical point are readily seen in the $T = 0$ plane of figure 2(*b*): there are three lines of first-order transitions OP, DP and CP which meet at a triple point P. The line OP separates phases denoted by $++$ and $--$, line CP separates phases $++$ and $+-$ and line DP separates phases $--$ and $+-$. In the $T = 0$ limit the magnetization is $+1$ (-1) in the $++$ $(--)$ phases while it assumes an intermediate value in the third $+-$ phase. The magnetization varies discontinuously on crossing the hatched surfaces in figure 2(*b*).

In order to determine whether the tricritical point is a *singular* feature of the $z \to \infty$ limit, we have studied numerically the recursion relation and magnetization for a Bethe lattice with $z = 6$. We follow a large ($N = 10\,000$) but finite sample of xs under iteration of equation (3) until an approximate fixed distribution is reached. The free energy per spin, for interior spins, is also evaluated in such a procedure to ensure that the system reaches a point of stable equilibrium. We map out the resulting phase diagram by looking for singular behaviour in m as h_0, h_1 and T are varied. Figure 3 shows a typical magnetization curve as a function of h_0 in the large h_1 limit. The discontinuity in m is a first-order transition accompanied by strong hysteresis effects.

We find a phase diagram in complete accord with the infinite z limit (figure 2(*b*)). Three sheets of first-order transitions separate three distinct phases $++$, $--$ and $+-$. The exact symmetry present when $h_0 = h_1$ results in a tricritical point. The new sheets of transitions, absent for $z = 3$, are not restricted to field values for which $\langle h_i \rangle = 0$. The magnetization at the corresponding critical points is also non-zero, as a consequence of symmetry breaking due to the field imbalance. In the limit of one of the field components becoming large, h_0 or $h_1 \to \infty$, the critical T associated with the transitions saturates at a *non-zero* value ($T_c/J \approx 2.2$).

The connection between these two seemingly distinct scenarios can be explored by investigating the effects of asymmetry in the field distribution. This can be achieved within the bimodal distribution, equation (2), by allowing $p \neq \frac{1}{2}$. In the case where a tricritical point is present for $p = \frac{1}{2}$, any slight asymmetry destroys the delicate balance required for three phases to become critical simultaneously. The tricritical point is then replaced by a critical end point†. However, in both cases ($z = 3$ and $z = 6$) we find that for $p \gg \frac{1}{2}$, the two scenarios in figures 2(*a*) and (*b*) are replaced by figure 4 (note the interchange of the h_0 and h_1 axes for ease of viewing). There is now a single sheet of first-order transitions bounded by a single critical line. The value of p which marks this change in the phase diagram topology is z-dependent. Thus, changes in either z or p have qualitative effects on the phase diagram topology.

† If there is no tricritical point for $p = \frac{1}{2}$, (figure 2(*a*)), there is no change in the phase diagram topology for any slight asymmetry.

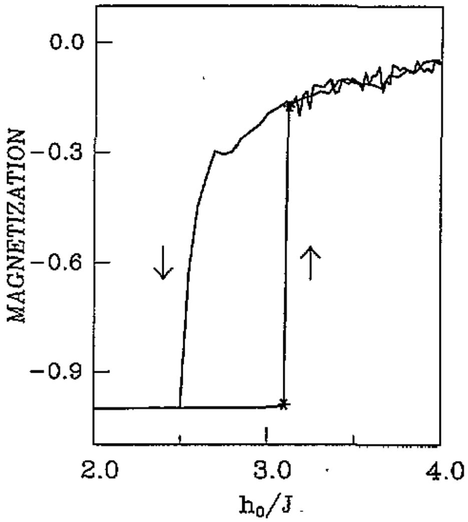

Figure 3. A typical magnetization curve as a function of h_0/J for a Bethe lattice with $z = 6$. A symmetric distribution of fields is considered at a low temperature and in the large-h_1 limit: $p = 0.5$, $T/J = 1.0$, $h_1/J = 10$. A hysteresis loop, formed by first increasing (lower branch) then decreasing (upper branch) h_0/J is indicative of a first-order transition. The upper branch is a metastable solution while multiple solutions are found in the region around the vertical portion of the curve. The position of the transition, found from evaluation of the free energy, is also indicated (*). At higher temperatures, both the discontinuity in m and the associated hysteresis loop are absent.

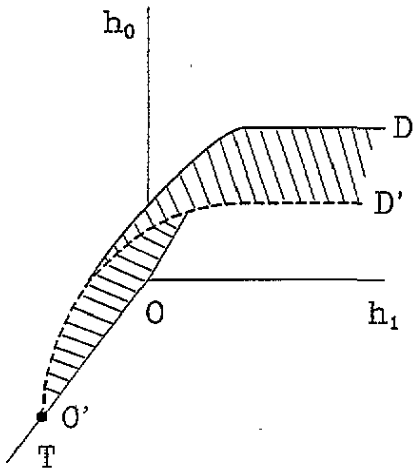

Figure 4. The schematic phase diagram for a Bethe lattice with $z = 3$ or $z = 6$ for $p \gg \frac{1}{2}$. A single sheet of first-order transitions is present (the hatched surface), bounded by a critical line O′D′. This line does *not* intersect the $T = 0$ plane.

We now present evidence that the RFIM on a 3D Euclidean lattice also shows some of these same phase diagram topologies. The key feature distinguishing between these distinct scenarios is the existence, or absence, of transitions at low temperatures in the limit of large h_0 or h_1. We have used a polynomial time-flow algorithm [16], first implemented in the study of the RFIM by Ogielski [14], to determine exactly the behaviour of the system at $T = 0$ in the limit $h_1 \to \infty$. We obtain numerically the ground states of the RFIM on cubic lattices of linear size L, ranging from $L = 4$ to 32, and calculate the disconnected susceptibility

$$\chi_L = \frac{1}{L^3} \sum_{\langle i,j \rangle} (\langle S_i S_j \rangle_c - \langle S_i \rangle_c \langle S_j \rangle_c) \tag{7}$$

as a function of h_0 and p for $h_1 = 10J$. Here, $\langle \ldots \rangle_c$ denotes the configurational averaging over different realizations of the fields (ranging from 10 000 samples for the smaller systems up to a few hundred for $L = 32$). Finite-size scaling considerations imply

$$\chi_L = L^{2-\bar{\eta}} f((h_0 - h_c) L^{1/\nu}) \tag{8}$$

with a first-order transition corresponding to $\bar{\eta} = -1$. In equation (8), h_c is the value of h_0 where a transition between the $--$ and $+-$ phases may take place.

Figure 5 is a log–log plot of the peak height, $\chi_{L,\max}$, as a function of L for two different values of p. In the symmetric case, $\chi_{L,\max}$ saturates for large L indicating the absence of any transition in the thermodynamic limit. However, for $p = 0.8$, $\chi_{L,\max}$ obeys scaling with $\bar{\eta} \approx -1$, which is consistent with a first-order transition. These findings suggest that for $p = \frac{1}{2}$, the resulting phase diagram is as in figure 2(a) while for large p it crosses over to figure 4, as in the Bethe lattice with coordination number $z = 3$.

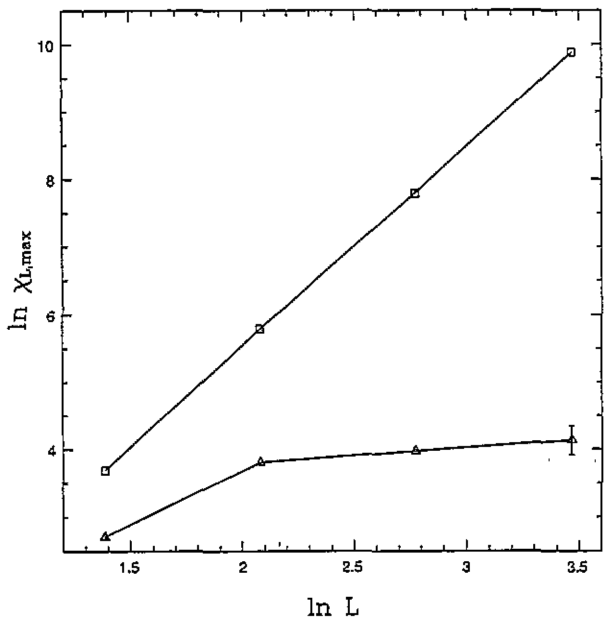

Figure 5. Size dependence of the peak height of the disconnected susceptibility for systems of up to 32^3 spins. The lower points (triangles) are for a symmetric $p = \frac{1}{2}$ distribution showing that $\chi_{L,\max}$ saturates for large L. The upper points (squares) are for an asymmetric distribution with $p = 0.8$. In this case, $\chi_{L,\max}$ is seen to obey scaling, equation (8), with $\bar{\eta} \approx -1$. Except for the largest symmetric system, typical error bars are smaller than the points plotted.

We finally provide a simple physical explanation for this surprising variation of random-field behaviour. The key point is whether or not the system can sustain transitions with broken Ising symmetry due to $\langle h_i \rangle \neq 0$. Consider the transitions at low temperatures predicted for large h_1 (figures 2(*b*) and 4) as h_0 is varied. In this limit, only the sites that experience a field h_0, which are a fraction p of the lattice, are free to fluctuate. A necessary condition for this transition to exist is that these sites form a connected cluster, i.e. $p > p_c$, the percolation threshold [17]. Increasing z or p favours the formation of an infinite cluster and allows for a first-order transition. In the case of a Gaussian distribution of random fields this percolation effect is no longer operative—a phase diagram with only two distinct phases is obtained.

Our calculations indicate that statistical correlations in the random-field distribution (eg. the connectedness of the sites having a given field value) can have a profound effect on the phase diagram topology and hence the nature of the random-field transitions [18]. A similar effect is to be expected in many experimental realizations of the RFIM. In the latter case, additional correlations introduced by the intrinsic structure of the system (eg. porous media†, surface preparation in dilute antiferromagnets [19]) may also play a role.

Acknowledgments

We are grateful to Neil Shrimpton, Wen-Jong Ma and especially Moses Chan for stimulating discussions. We are indebted to Andy Ogielski for providing us with several preprints that enabled us to learn how to determine the ground states of the RFIM efficiently. This work was supported by grants from NASA, NATO, NSF, ONR, the Donors of the Petroleum Research Fund administered by the American Chemical Society, the Polish agency KBN, the Center for Academic Computing at Penn State, and Instituto Nazionale di Fisica Nucleare INFN, sezione di Padova.

References

[1] For recent reviews, see Natterman T and Rujan P 1989 *Int. J. Mod. Phys.* B **3** 1597
Fisher D S, Grinstein G M and Khurana A 1988 *Physics Today* **41** 58
[2] Fishman S and Aharony A 1979 *J. Phys. C: Solid State Phys.* **12** L729
Wong P Z, von Molnar S and Dimon P 1982 *J. Appl. Phys.* **53** 7954
Cardy J 1984 *Phys. Rev.* B **29** 505
Birgenau R J, Cowley R A, Shirane G and Yoshizawa H 1982 *Phys. Rev. Lett.* **48** 1050
Hill J P, Thurston T R, Erwin R W, Ramsted M J and Birgeneau R J 1991 *Phys. Rev. Lett.* **66** 3281
Grest G S, Soukoulis C M and Levin K 1986 *Phys. Rev.* B **33** 7659
[3] Maher J V, Goldburg W I, Pohl D W and Lanz M 1984 *Phys. Rev. Lett.* **53** 60
Goh M C, Goldburg W I and Knobler C M 1987 *Phys. Rev. Lett.* **58** 1008
Wiltzius P, Dierker S B and Dennis B S 1989 *Phys. Rev. Lett.* **62** 804
[4] Wong A and Chan M H W 1990 *Phys. Rev. Lett.* **65** 2567
[5] de Gennes P G 1984 *J. Phys. Chem.* **88** 6469
[6] Schneider T and Pytte E 1977 *Phys. Rev.* B **15** 1519
For a general analysis see Aharony A 1978 *Phys. Rev.* B **18** 3318
[7] Bruinsma R 1984 *Phys. Rev.* B **30** 289
[8] McKay S R and Berker A N 1988 *J. Appl. Phys.* **64** 5785

† For a liquid–vapour transition in a porous medium (PM) [4], the $++$, $--$ and $+-$ phases correspond to liquid filling the PM, vapour filling the PM and vapour inside the PM except for a liquid layer at the walls of the PM, respectively.

McKay S R and Berker A N 1989 *New Trends in Magnetism* ed M D Coutinho-Filho and S M Rezende (Singapore: World Scientific)
Cao M S and Machta J *Preprint*
[9] Ogielski A T and Huse D A 1986 *Phys. Rev. Lett.* **56** 1298
[10] Bray A J and Moore M A 1985 *J. Phys. C: Solid State Phys.* **18** L927
Villain J 1985 *J. Physique* **46** 1843
Fisher D S 1986 *Phys. Rev. Lett.* **56** 416
[11] Houghton A, Khurana A and Seco F J 1985 *Phys. Rev. Lett.* **55** 856
[12] Young A P and Nauenberg M 1985 *Phys. Rev. Lett.* **54** 2429
[13] Andelman D 1983 *Phys. Rev.* B **27** 3079
Maritan A, Swift M R, Cieplak M, Chan M H W, Cole M W and Banavar J R 1991 *Phys. Rev. Lett.* **67** 1821
Kaufman M, Klunzinger P E and Khurana A 1986 *Phys. Rev.* B **34** 4766
Horiguchi T 1979 *J. Math. Phys.* **20** 1774
[14] Ogielski A 1986 *Phys. Rev. Lett.* **57** 1251 Ogielski has determined the exact ground states of the RFIM in three dimensions for system sizes up to 32^3 spins. He finds clear evidence of the first scenario for a Gaussian distribution of fields, whereas his study of the bimodal model is not conclusive.
[15] Griffiths R B 1969 *Phys. Rev. Lett.* **23** 17
[16] Goldberg A V 1985 *MIT Report (November)*
[17] The connection between the random-field Ising model and the percolation problem was noted by Domb C and Entin-Wohlman O 1984 *J. Phys. A: Math. Gen.* **17** L1
[18] Imry Y and Ma S K 1975 *Phys. Rev. Lett.* **35** 1399 Such correlations are not taken into account in a conventional Imry–Ma argument and may affect the value of the lower critical dimension.
[19] Hill J P, Feng Q, Birgeneau R J and Thurston T R 1991 *Phys. Rev. Lett.* **66** 3281; *Preprint*